EVOLUTION OF NEUROENDOCRINE CELL POPULATION AND PEPTIDERGIC INNERVATION, ASSESSED BY DISCRIMINANT ANALYSIS, DURING POSTNATAL DEVELOPMENT OF THE RAT PROSTATE

ROSARIO RODRÍGUEZ[1], JOSÉ M POZUELO[1], ALFREDO SÁNCHEZ ALBERCA[2], RIÁNSARES ARRIAZU[1], JOSÉ M CÁRDENAS[2], ILDEFONSO INGELMO[3], ROCÍO MARTÍN[4] AND LUIS SANTAMARÍA[5]

[1]Department of Physiology, Morphology, and Nutritional Sciences, San Pablo University, Madrid, Spain; [2]Department of Quantitative Methods, San Pablo University, Madrid, Spain; [3]Department of Anaesthesiology, Hospital Ramón y Cajal, Madrid, Spain; [4]Service of Pathology, Hospital N. Sra de Sonsoles, Ávila, Spain; [5]Department of Anatomy, Histology, and Neuroscience, School of Medicine, Autonomous University of Madrid, Madrid, Spain
e-mail: luis.santamaria@uam.es
(Accepted. February 21, 2007)

ABSTRACT

Serotonin immunoreactive neuroendocrine cells and peptidergic nerves (NPY and VIP) could have a role in prostate growth and function. In the present study, rats grouped by stages of postnatal development (pre-pubertal, pubertal, young and aged adults) were employed in order to ascertain whether age causes changes in the number of serotoninergic neuroendocrine cells and the length of NPY and VIP fibres. Discriminant analysis was performed in order to ascertain the classificatory power of stereologic variables (absolute and relative measurements of cell number and fibre length) on age groups. The following conclusions were drawn: a) discriminant analysis confirms the androgen-dependence of both neuroendocrine cells and NPY-VIP innervation during the postnatal development of the rat prostate; b) periglandular innervation has more relevance than interglandular innervation in classifying the rats in age groups; and c) peptidergic nerves from ventral, ampullar and periductal regions were more age-dependent than nerves from the dorso-lateral region.

Keywords: androgen-dependence, discriminant analysis, neuroendocrine cells, NPY, peptidergic fibres, rat prostate, serotonin, VIP.

INTRODUCTION

The regulation of prostate growth has been considered as an almost exclusive function of the endocrine system. Nevertheless, the finding of cholinergic and adrenergic receptors in human prostate, and the presence of abundant autonomic neuroendings, suggest a role for innervation in homeostasis, growth and prostate function (McVary *et al.*, 1994; McVary *et al.*, 1998; Mottet *et al.*, 1999). In fact, the transduction signalling of neurotransmitters might modulate the growth and physiology of the prostate gland (McVary *et al.*, 1998; Farnsworth, 1999), while experimental denervation causes the loss of prostate function and atrophy (Lujan *et al.*, 1998).

Neuropeptides have been detected in the prostate of several species (mice, hamster, guinea pig, rabbit, rat and man); these substances might be also related to the growth, maintenance and function of the prostate. Non-cholinergic, non-adrenergic neurotransmitters could modulate the activity of androgens by transduction signalling (Adrian *et al.*, 1984; Lange *et al.*, 1990; Crowe *et al.*, 1991; Gkonos *et al.*, 1995; Jen *et al.*, 1996). Neuropeptide Y (NPY), and vasoactive intestinal polipeptides (VIP) have been especially well studied in relation to prostate function (Rodriguez *et al.*, 2005).

On the other hand, recent studies show that certain neuropeptides could be implicated in the development of proliferative prostate pathologies such as benign prostate hyperplasia (BPH) and prostate carcinoma. For example, VIP could induce cell proliferation of the acini in rat prostate (Juarranz *et al.*, 2001).

The function of the neuroendocrine cells described in the rat prostate could be related to the excretion of prostate secretions toward the urethra, and these cells

might be regulated by androgens (Rodriguez *et al.*, 2003). Recently, several studies have claimed that neuroendocrine cells from human prostate could be implicated in the pathogenesis of BPH (Martin *et al.*, 2000) and in prostate cancer (Cohen *et al.*, 1991; di Sant'Agnese, 1992; Abrahamsson, 1999). Moreover, certain peptides might be implicated in the growth and development of the prostate, *e.g.*, VIP could induce cell proliferation of acini from rat prostate.

There is evidence of morphological and functional relationships between neuroendocrine cells and prostate nerve fibres, resulting in a neuro-hormonal system that might modulate androgenic action in the prostate (Wanke *et al.*, 1990; Abdul *et al.*, 1995; Gkonos *et al.*, 1995).

The combined use of immunohistochemistry and unbiased stereologic methods will be interesting in establishing quantitative relationships among the diverse types of peptidergic nerves and neuroendocrine cells from rat prostate in postnatal development (Rodriguez *et al.*, 2003; 2005).

The present study aims to: a) evaluate the amount and distribution of nerve fibres immunoreactive to Protein Gene Product 9.5 (PGP 9.5), NPY and VIP, and of immunoreactive Serotonin (SER) neuroendocrine cells in several regions of the rat prostate during postnatal development; b) quantify the correlation between peptidergic innervation and the neuro-endocrine cell population and its changes in postnatal development; and c) provide evidence of the value of quantitative parameters of both nerve fibres and neuroendocrine cells as relevant in distinguishing rat prostates of different ages.

MATERIALS AND METHODS

ANIMALS

The study was carried out on 68 Wistar male rats. The animals were distributed into 4 groups according to postnatal development: prepubertal (15 days old), pubertal (30 days old), young adult (90 days old) and aged adult (540 days old). Animal protocols agreed with the guidelines for the care and use of research animals adopted by the Society for the Study of Reproduction. All rats were killed by exsanguination after CO_2 narcosis. The prostate complex was dissected from the abdominal cavity of each animal and exhaustively cut into 2-mm-thick slices. The section plane was perpendicular to the saggital axis of the gland. All specimens were fixed by immersion in 10% paraformaldehyde in phosphate buffered saline (PBS) with pH 7.4 for 24 h and then embedded in paraffin.

SAMPLING PROCEDURE

For each prostate, all slices obtained were embedded in a paraffin block. The blocks were then serially sectioned. Five μm-thick sections (for immuno-histochemistry and routine haematoxyline-eosine techniques) alternating with 10 μm-thick sections (for stereological methods) were performed for each block. All prostate regions were included in every section.

For the evaluation of immunohistochemical and stereological studies, twenty sections were selected by random systematic sampling (Gundersen *et al.*, 1981) from each block obtained from each animal.

IMMUNOHISTOCHEMISTRY

Nerve fibres immunoreactive to PGP 9.5, NPY and VIP, and neuroendocrine cells immunoreactive to SER, were studied in duct, ampullar, dorsal and ventral rat prostate regions from pubertal (P), young adult (A), and aging adult (AA) animals. In pre-pubertal (PP) animals the morphologic identification of the ampullar, dorsal and ventral regions was not yet reliable; then, all the immunohistochemical and quantitative studies were performed in two different zones: the prostate (including the three undifferentiated ventral, dorsal and ampullar regions) and the duct zone (easily identified throughout all the age groups).

PGP 9.5 was used as a general marker for nerve fibres, NPY and VIP as markers for peptidergic innervation and SER as a neuroendocrine cell marker.

For each antigen employed, the immunoreactive nerve fibres were evaluated in periglandular (Pg) and interglandular (Ig) compartments from dorsal, ampullar and ventral prostate in P, A and AA animals, and the prostate zone in PP animals. The Pg zone was defined as a band 10 μm wide around the acini, and the remaining stroma was considered as an Ig zone. In order to evaluate ductal innervation, a periductal zone (Pd) with an extension of 20 μm (including the periductal muscular layer) around the excretory ducts was also considered. The abbreviations employed are summarised in Table 1.

2

Table 1. *List of abbreviations.*

PGP 9.5	Protein Gene Product 9.5
NPY	Neuropeptide Y
VIP	Vasoactive Intestinal Peptide
SER	Serotonin
PP	Pre-pubertal
P	Pubertal
A	Young Adults
AA	Aging Adults
Pg	Periglandular compartment
Ig	Interglandular compartment
Pd	Periductal compartment

At least three selected slides per animal (per prostate) and per antigen were immunostained in all the animal groups. Deparaffinised and rehydrated tissue sections were treated for 30 min with 0.3% hydrogen peroxide in phosphate-buffered saline (PBS), pH 7.4, to block endogenous peroxidase. To detect PGP 9.5 immunoreactivity, sections were incubated with a monoclonal anti-PGP 9.5 antibody (Biomeda, Foster City, CA, USA) at a dilution of 1:25. To detect SER, NPY and VIP immunoreactivity, sections were incubated respectively with a polyclonal anti-SER antibody (Biomeda) at a dilution of 1:25, polyclonal anti-NPY antibody (Hammersmith Hospital London, UK) at a dilution of 1:1000, and polyclonal anti-VIP antibody (Biomeda) at a dilution of 1:2. All primary antisera were diluted in PBS pH 7.4 containing 1% bovine serum albumin (BSA) plus 0.1% sodium azide. All incubations with primary antisera were left overnight at 4ºC. The second antibody used for the primary monoclonal antibody was a biotin-caproyl-anti-mouse immunoglobulin (Biomeda). The second antibody used for primary polyclonal antibodies was a biotin-caproyl-anti-rabbit immunoglobulin (Biomeda). Both were diluted at 1:400 in PBS containing 1% BSA without sodium azide. The tissues were incubated for 30 min at room temperature. Thereafter, sections were incubated with a streptavidin-biotin-peroxidase complex (Biomeda). The immunostaining reaction product was developed using 0.1 g diaminobenzidine (DAB) (3,3',4,4' - tetraminobiphenyl, Sigma, St Louis, USA) in PBS (200 ml), plus 40 μl of hydrogen peroxide.

After immunoreaction, sections were counter-stained with methyl green for nerve fibre studies, and Harris hematoxyline for neuroendocrine cell studies. All slides were dehydrated in ethanol and mounted in a synthetic resin (Depex, Serva, Heidelberg, Germany). The specificity of the immunohistochemical procedures was checked by incubation of sections with nonimmune serum instead of the primary antibody.

STEREOLOGICAL METHODS

1. Evaluation of numerical density of SER immuno-reactive cells (N_V) (number of SER immunoreactive cells per unit volume). The optical disector, an unbiased stereological method (Bjugn *et al.*, 1993; Wreford, 1995; Mayhew *et al.*, 1996), was employed. Briefly, the procedure used was as follows. Three 10-μm-thick sections serotonin immunostained per animal (per prostate) were chosen by systematic random sampling. Such section thickness is obligatory for the optical disector method (Mayhew and Gundersen, 1996).

Only the prostate zone of the periurethral ducts in all age groups was scanned in order to count cells, given that no SER immunoreactive cells were found in the other prostate regions. An average of 100 fields per section were systematically randomly sampled. All measurements were performed using an Olympus microscope with a ×100 objective (numerical aperture 1.4) at a final magnification of ×1200. The microscope was connected to a video camera and supplied with a motorised stage connected to a computer. The software used (Stereologic Software Package, CAST-GRID; Interactivision, Silkeborg, Denmark) commands the XY movement of the stage and allows the automatic selection of microscopic fields (Martin *et al.*, 1997). The program generates the disector grid that was superimposed on the microscopic image captured by the video camera and displayed on the monitor. The disector volume (Vdis) was calculated using the formula:

$$Vdis = Sd \cdot Hd$$

where Sd = 1312 μm^2 (area of the disector frame), Hd = 5 μm, which is the distance between the two focal planes chosen for determining the disector volume in the tissue section; this distance was measured by means of a microcator (Heidenhain; Traunreut, Germany) connected to the Z displacement of the microscope stage. Because the total thickness of the section was 10 μm, a space of 2.5 μm above and below the optical section was maintained to avoid artefacts produced in the physical surface of the section. The volume of the disector (Vdis) was thus 6560 μm^3.

The SER immunoreactive cells eligible to be counted were determined by using Sterio's convention (Sterio, 1984); only those cells that appeared in the upper focal plane and that were not observed in the lower focal plane were counted (Q_d^-). The numerical density of SER immunoreactive cells, or SER immuno-reactive cell number per unit volume (N_V), was then obtained by the formula:

$$N_V = \Sigma\, Q_d^- / \Sigma\, Vdis \cdot F_R$$

where $\Sigma\, Vdis$ = total sum volume of disectors applied in each selected section. N_V was calculated as the number of cells per mm^3 of prostate volume.

Changes in volume during tissue processing were calculated in order to transform the volumes that were measured in paraffin-embedded material to their actual measurements in fresh prostate. The amount of shrinkage (F_R) was previously calculated (Martin *et al.*, 2001). In brief, fresh prostate volume (Vprost) was obtained by water immersion of unfixed specimens. The differences between fresh volumes and Cavalieri-estimated volumes (Mayhew, 1991) for the whole organ were obtained, and the percentage of shrinkage was calculated. On average, a 32% reduction in the volume of fresh tissue by processing the samples was found. Consequently, an $F_R = 1.3$ was applied in calculating the number of SER immunoreactive cells to adjust prostate volume for shrinkage.

2. Evaluation of SER immunoreactive cell number per prostate (N). This was calculated by multiplying the corresponding N_V SER immunoreactive cells by the volume of the periurethral ducts (Vducts). $N = N_V \cdot Vducts$.

To obtain Vducts, the fraction of prostate volume contained in the periurethral duct (V_V ducts) was measured, *i.e.*, the ratio between the periurethral duct area and the reference area of prostate tissue. This volume fraction was estimated in an average of 30 systematically randomly sampled microscopic fields (an average of 194000 μm^2 per field) in five systematically randomly selected sections of each animal from each group. The measurements were performed by counting the points hitting either the periurethral duct area or the reference area, using the CAST-GRID software package, which provides a counting point frame with a point-associated area $A(p) = 45\ \mu m^2$ (Martin *et al.*, 2000). The final magnification for these measurements was ×500. Vduct was then calculated by multiplying V_V duct by Vprost.

3. Evaluation of length fibre density (L_V) immunoreactive to PGP 9.5, NPY and VIP: length of immunoreactive fibre per unit volume. The L_V of PGP 9.5, NPY and VIP immunostained fibres was evaluated in the Pg and Ig compartments for ventral, dorsal, ampullar and acini regions, and in the Pd compartment for the ductal region, for each age group defined above. The stromal and epithelial compartments together were considered as a reference space. Briefly, the procedure used was as follows. Three 10-μm-thick

PGP 9.5, NPY and VIP immunostained sections per animal (per prostate) were chosen by systematic random sampling. For all practical purposes, biological microstructures such as capillaries, tubules and axons can be regarded as linear features. The most important stereological attribute of linear features is their L_V, *i.e.*, total line length per unit volume from which absolute length can be calculated, provided the reference volume is known (Mayhew, 1991). The nerve profile was defined as the portion of immuno-stained nerve segment seen, regardless of its size and length. An isotropic distribution of the nerve fibres was assumed in this study (Howard and Reed, 2005).

An average of 100 fields per section in each prostate zone were systematically randomly sampled and used to count the number of immunoreactive nerve profiles. All measurements were performed with the same equipment and magnifications that were employed to estimate the number of neuroendocrine cells immunostained to SER.

The nerve profiles were counted with an unbiased counting frame according to the unbiased counting rule(Gundersen *et al.*, 1988). They were designated as Q^-.

L_V was a calculated using the formula:

$$L_V = (2 \cdot \Sigma Q^-) / \Sigma A$$

where Q^- = number of immunopositive nerve profiles counted with the unbiased counting frame and ΣA = total area sampled, *i.e.,* the area of the frame (1312 μm^2) multiplied by the number of selected fields.

4. Evaluation of the length of fibres immunoreactive to PGP 9.5, NPY and VIP per prostate (L). The L PGP 9.5, NPY and VIP was calculated by multiplying their corresponding L_V by the volume of each region.

To obtain regional volume, the fraction of prostate volume contained in each region (V_V amp , V_V dor , V_V vent and V_V duct) was measured, *i.e.*, the ratio between ampullar, dorsal, ventral and periurethral duct areas, and the reference area of prostate tissue. This volume fraction was estimated for an average of 30 systematically randomly sampled microscopic fields (an average of 194000 μm^2 per field) in five systematically randomly selected sections of each animal from each group. The measurements were performed by counting the points hitting either the ampullar, dorsal, ventral, acini or periurethral duct areas, and the reference area, using the CAST-GRID software package, which provides a counting point frame with a point-associated area $A(p) = 45\ \mu m^2$ (Martin *et al.*, 2000). The final magnification for these

4

measurements was ×500. The regional volumes (V amp, V dor, V vent and V duct) were then calculated by multiplying each V_V by prostate volume (Vprost).

5. Evaluation of prostate volume in pre-pubertal rats. Because of the small size of the prostate complex in this group, it was not possible to apply the water displacement method in order to estimate glandular volume. Therefore, the Cavalieri principle was employed. Each paraffin block was exhaustively cut into serial sections 7 μm thick, and then from each set of 10 sections 1 was collected and stained with haematoxylin-eosin. The Cavalieri estimator (Gundersen *et al*., 1988) was then applied to these sections, and the volume of the pre-pubertal prostate was obtained using the formula:

$$\text{Vprost PP} = t \bullet a_p \bullet \Sigma\, p \bullet F_R$$

where Vprost PP = Volume of the pre-pubertal prostate (mm^3); t = average thickness from each set of 10 sections (0.07 mm) = 7 μm × 10; a_P = Point-associated area of the counting grid employed (0.25 mm^2); $\Sigma\, p$ = Total number of grid points hitting each section; F_R = Amount of shrinkage (1.3)

STATISTICAL ANALYSIS

All estimates were expressed as mean ± CI (confidence intervals at 95%) for each prostate region and age group. In order to determine the variables that most accurately classify rats in the groups of development being considered, stepwise linear discriminant analysis was applied to the age groups for different sets of variables: regional (relative or absolute) and global (relative or absolute) measurements. Discriminant variables were selected according to Wilks' lambda: at each step, the variable that minimises the overall Wilks' lambda or maximises the associated F statistic is selected (F to enter = 3.84 and F to remove = 2.71). Wilks' lambda statistic explains the rate of total variability that is not due to differences among groups. A lambda of 1 means that the mean of the discriminant scores is the same in all groups and there is no variability between groups, while a lambda near 0 means that there is a significant difference among groups. Therefore, Wilks' lambda provides a test of the null hypothesis that the population means are equal. The larger lambda is, the less discriminating power is present (Hair *et al*., 1998). Discriminant analysis assumes that the variables are jointly normally distributed; therefore, data were preprocessed by applying logarithmic transformations to quantitative variables to fit them to normal distributions and substituting missing values with the age-group mean

so as to avoid reduction of sample size. Statistical analyses were performed using the SPSS package (Chicago, Inc. III USA 1995). The level of significance for all tests employed was p < 0.05.

RESULTS

SER immunoreactive cells were located between the epithelial cells of the periurethral prostate ducts in all age groups (Fig. 1a,b). PGP 9.5, NPY and VIP immunoreactive fibres were detected at Pg and Ig compartments in all prostate regions (ventral, dorsal, ampular), and around the periurethral prostate ducts (Pd) in all development groups (Fig. 1c-f).

The discriminant analysis for relative measurements, irrespective of prostate region, *i.e.*, including pre-pubertal animals, reveals that the most discriminant variables were, in order of classificatory power:

1-Nv SER, increasing from the pre-pubertal group to pubertal animals, and then decreasing during adult life.

2-Lv NPY (Pg), increasing from the pre-pubertal group to pubertal animals, and then decreasing during adult life.

3-Lv VIP (Pg), increasing from the pubertal group to adult animals.

With these variables in the model, 88.2% of individuals were correctly classified. Table 2 shows the significant reduction of the Wilks' lambda statistic with these variables included in the model. The estimates of mean values ± CI of these variables are displayed in Fig. 2.

Discriminant analysis of relative measurements considering their regional distribution illustrates that the most discriminant variables were, in order of classificatory power:

1-N_V SER in the ducts region.

2-L_V NPY (Pg) in the ventral region.

3-L_V NPY (Pg) in the ampullar region.

4-L_V VIP (Pg) in the ventral region.

With these variables in the model, 87.7% of individuals were correctly classified. Table 3 shows the significant reduction of the Wilks' lambda statistic with these variables included in the model. The variation of these variables related to age group are identical to those indicated for relative measurements irrespective of prostate region (Fig. 3).
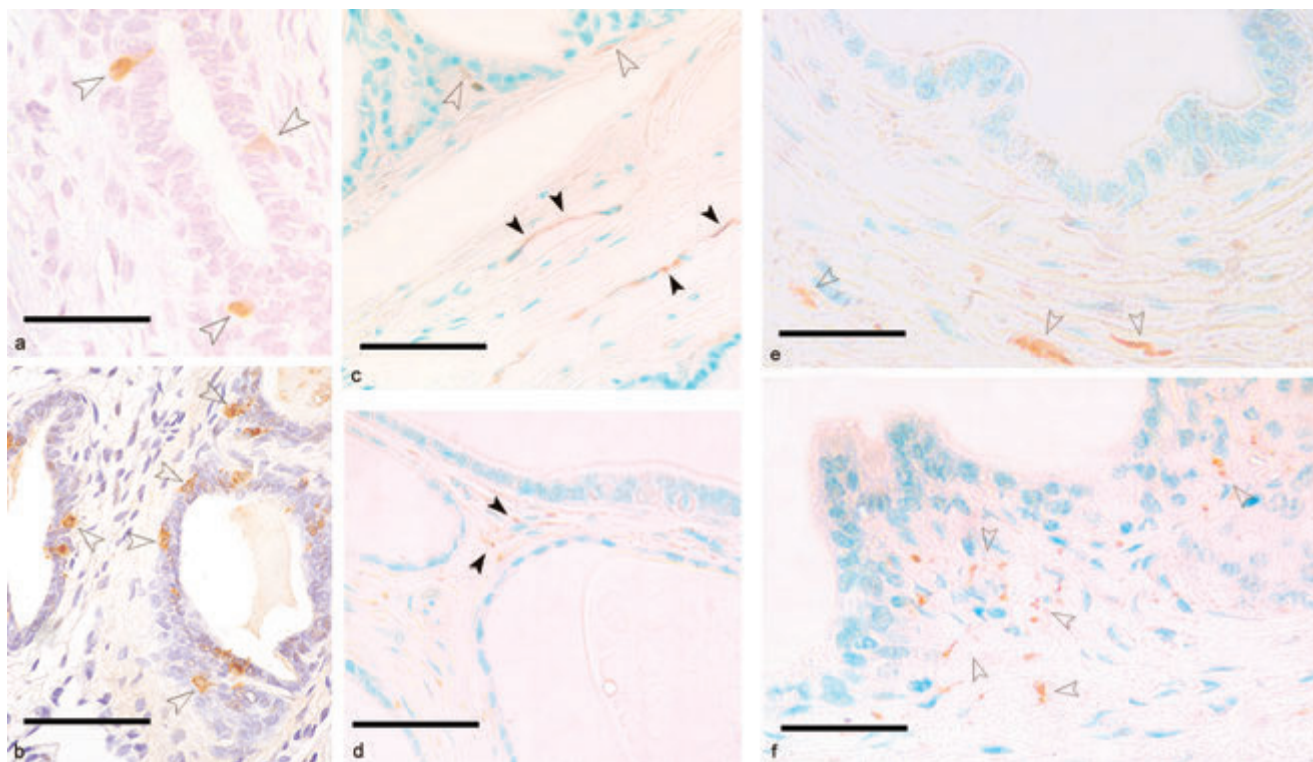
Fig. 1. *a) Periurethral duct from a pre-pubertal rat prostate. Some neuroendocrine cells immunostained for serotonin (empty arrow-heads) are visible. Bar calibration: 20 μm. b) Same localisation as in (a) in a young adult rat; abundant neuroendocrine serotonin immunoreactive cells (empty arrow-heads) are detected. Bar calibration: 14 μm. c) Interglandular (black arrow-heads) and periglandular (empty arrow-heads) nerve fibres immunostained for PGP 9.5 are shown in the ventral region of an aged adult rat prostate. Bar calibration: 14 μm. d) Interglandular (black arrow-heads) immunoreactive NPY neuroendings from the ampullar region of a young adult rat. Bar calibration: 14 μm. e) Scarce VIP immunostained nerve fibres observed in periductal localisation (empty arrow-heads) in a prostate from a pubertal rat. Bar calibration: 20 μm. f) Abundant VIP immunostained nerve fibres observed in periductal localisation (empty arrow-heads) in a prostate from a young adult rat. Bar calibration: 20 μm.*

Table 2. *Discriminant analysis of relative measurements without considering prostate regions (including pre-pubertals).*

Entered variable [1]	Wilks' lambda[2]	F[3]	P[4]
N_V SER	0.378	35.150	0.000
L_V NPY (Pg)	0.226	23.195	0.000
L_V VIP (Pg)	0.107	25.335	0.000

[1]All variables were logarithmically transformed. [2]This column shows the Wilks' lambda for every variable entered. [3]F distribution of Snedecor, the F minimum value for entering the variables was 3.84. [4]Level of significance $p < 0.05$.

Table 3. *Discriminant analysis for regional relative measurements.*

Entered variable [1]	Region	Wilks' lambda[2]	F[3]	P[4]
N_V SER	Ducts	0.347	50.767	0.000
L_V NPY (Pg)	Ventral	0.238	27.812	0.000
L_V NPY (Pg)	Ampullar	0.185	22.922	0.000
L_V VIP (Pg)	Ventral	0.152	19.957	0.000

[1]All variables were logarithmically transformed. [2]This column shows the Wilks' lambda for every variable entered. [3]F distribution of Snedecor, the F minimum value for entering the variables was 3.84. [4]Level of significance $p < 0.05$.
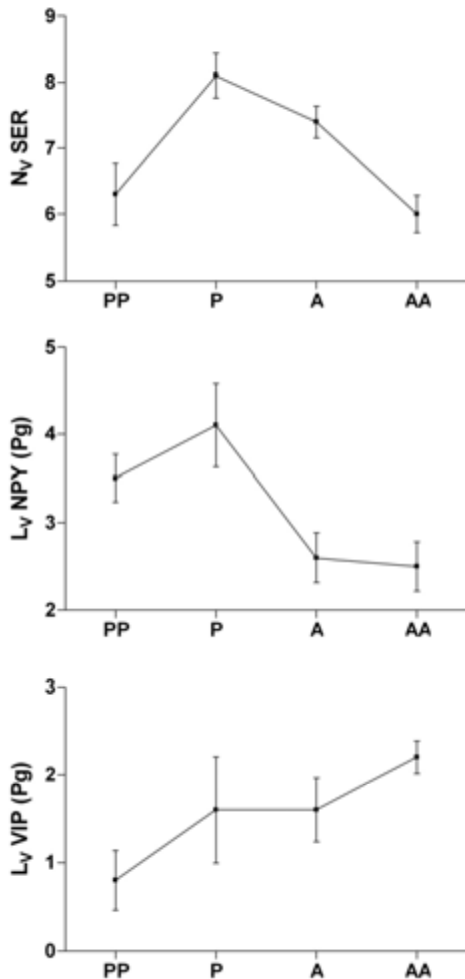
Fig. 2. *Graphics showing the evolution of stereological variables during development. The graphics are ordered from top to bottom on the figure according to their classificatory power in discriminant analysis for relative measurement without considering the prostate regions. The values are logarithmically transformed and expressed as mean ± CI. N_V SER: Numerical density of serotonin immunostained neuroendocrine cells (number of cells per mm^3 of ductal epithelium). L_V NPY (Pg): Length density of periglandular NPY immunoreactive fibres (length fibre per mm^2 of stromal tissue). L_V VIP (Pg): Length density of periglandular VIP immunoreactive fibres (length fibre per mm^2 of stromal tissue). PP: prepubertal group; P: pubertal group; A: young adult group; AA: aged adult group.*
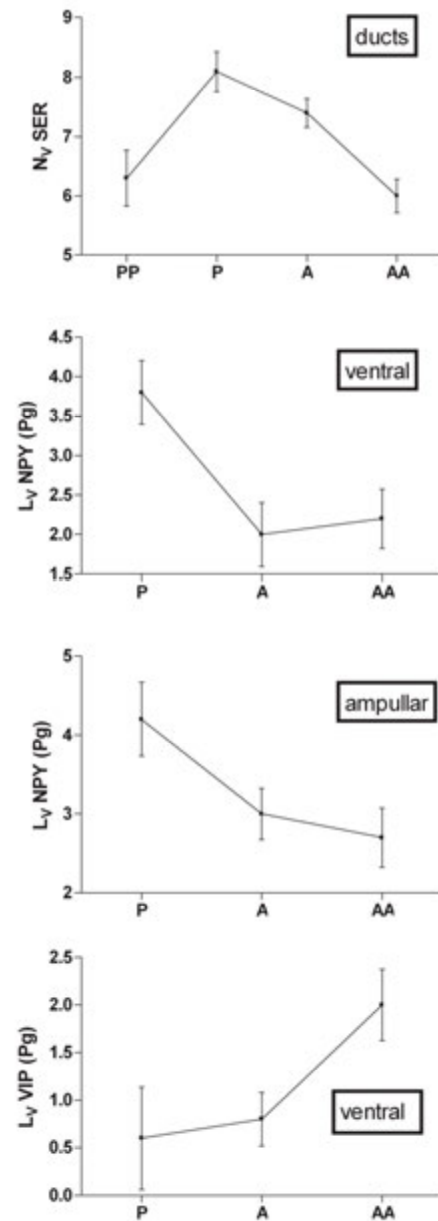

Fig. 3. *Graphics showing the evolution of stereological variables during development. The graphics are ordered from top to bottom on the figure according to their classificatory power in discriminant analysis for relative measurement considering their regional distribution. The values were logarithmically transformed and expressed as mean ± CI. N_VSER: Numerical density of serotonin immunostained neuroendocrine cells (number of cells per mm^3 of ductal epithelium). L_V NPY (Pg): Length density of periglandular NPY immunoreactive fibres (length fibre per mm^2 of stromal tissue) in both ventral and ampular regions. L_V VIP (Pg): Length density of periglandular VIP immunoreactive fibres (length fibre per mm^2 of stromal tissue) in the ventral region. PP: pre-pubertal group; P: pubertal group; A: young adult group; AA: aged adult group.*

The discriminant analysis for absolute measurements irrespective of prostate regions, *i.e.*, including pre-pubertal animals, shows that the most discriminant variables are, in order of classificatory power:

1-L VIP (Pg), increasing from pre-pubertal animals to aged adults.

2-N SER, increasing from pre-pubertal to adults, and then decreasing slightly to aged adults.

3-L NPY (Pg), increasing from pre-pubertal to pubertal rats, and then maintaining pubertal values during adult life.

4-L PGP 9.5 (Ig), increasing from pre-pubertal animals to aged adults.

With these variables in the model, 82.4% of individuals were correctly classified. Table 4 shows the significant reduction of the Wilks' lambda statistic with these variables included in the model. The estimates of mean values ± CI of these variables are expressed in Fig. 4.

The discriminant analysis for absolute measurements considering their regional distribution shows that the most discriminant variables were, in order of classificatory power:

1-L VIP (Pd) in the ducts region, increasing from pre-pubertal animals to aged adults.

2-L VIP (Pg) in the ventral region, increasing from pubertal animals to aged adults.

3-N SER in the ducts region, increasing from pre-pubertal to adults, and then decreasing to aged adults.

4-L VIP (Ig) in the ampullar region. Unchanged from pubertals to young adults, and then increasing to aged adults.

With these variables in the model, 87.7% of individuals were correctly classified. Table 5 shows the significant reduction of the Wilks' lambda statistic with these variables included in the model. The estimates of mean values ± CI of these variables are expressed in Fig. 5.

Table 4. *Discriminant analysis of absolute measurements without considering prostate regions (including pre-pubertals).*

Entered variable[1]	Wilks' lambda[2]	F[3]	P[4]
L VIP (Pg)	0.945	203.073	0.000
N SER	0.047	76.360	0.000
L NPY (Pg)	0.031	52.780	0.000
L PGP 9.5 (Ig)	0.024	42.106	0.000

[1]All variables were logarithmically transformed. [2]This column shows the Wilks' lambda for every variable entered. [3]F distribution of Snedecor, the F minimum value for entering the variables was 3.84. [4]Level of significance $p < 0.05$.

Table 5. *Discriminant analysis for regional absolute measurements.*

Entered variable[1]	Region	Wilks' lambda[2]	F[3]	P[4]
L VIP (Pd)	Ducts	0.294	64.812	0.000
L VIP (Pg)	Ventral	0.205	32.023	0.000
N SER	Ducts	0.153	27.014	0.000
L VIP (Ig)	Ampullar	0.121	23.944	0.000

[1]All variables were logarithmically transformed. [2]This column shows the Wilks' lambda for every variable entered. [3]F distribution of Snedecor, the F minimum value for entering the variables was 3.84. [4]Level of significance $p < 0.05$.
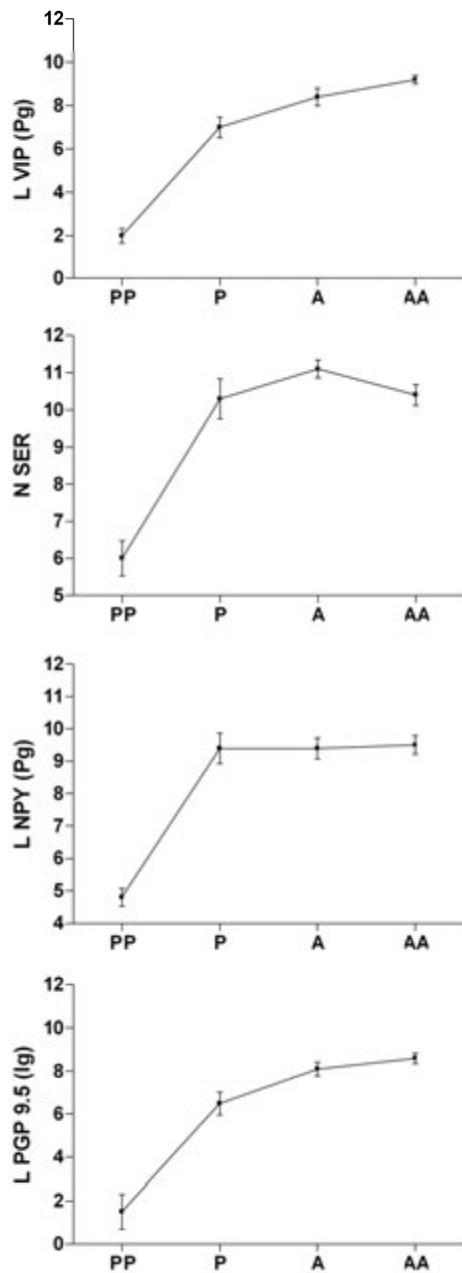
Fig. 4. *Graphics showing the evolution of stereological variables during development. The graphics are ordered from the top to the bottom of the figure according to their classificatory power in discriminant analysis for absolute measurement without consider the prostate regions. The values are logarithmically transformed and expressed as mean ± CI. L VIP (Pg): Absolute length of periglandular VIP immunoreactive fibres (mm). N SER: Absolute number of serotonin immunostained neuroendocrine cells. L NPY (Pg): Absolute length of periglandular NPY immunoreactive fibres (mm). L PGP 9.5 (Ig): Absolute length of interglandular PGP 9.5 immunoreactive fibres (mm). PP: pre-pubertal group; P: pubertal group; A: young adult group; AA: aged adult group.*
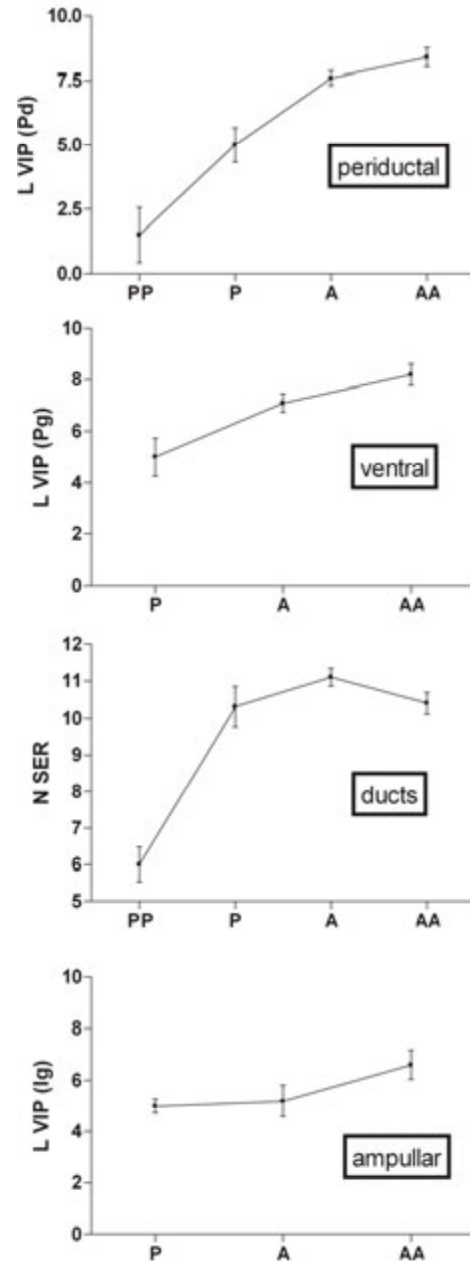
Fig. 5. *Graphics showing the evolution of stereological variables during development. The graphics are ordered from the top to the bottom of the figure according to their classificatory power in discriminant analysis for absolute measurement considering their regional distribution. The values were logarithmically transformed and expressed as mean ± CI. L VIP (Pd): Absolute length of periductal VIP immunoreactive fibres (mm). L VIP (Pg): Absolute length of periglandular VIP immunoreactive fibres (mm) in ventral region. N SER: Absolute number of serotonin immunostained neuroendocrine cells. L VIP (Ig): Absolute length of interglandular VIP immunoreactive fibres (mm) in the ampular region. PP: pre-pubertal group; P: pubertal group; A: young adult group; AA: aged adult group.*

DISCUSSION

The discriminant analyses employed in the present study highlight relevant correlations among ductal neuroendocrine cells and prostate innervation during postnatal development. Absolute and relative numbers of ductal neuroendocrine cells are relevant in order to classify the rats according to age group. The increase of these cells was related to the onset of puberty and their decline with aging. These findings might suggest androgenic modulation for the development of this cell population (Rodriguez *et al*., 2003). The innervation of the prostate compartments close to the epithelium (periglandular and periductal) was more relevant for classifying the rats by age than interglandular (stromal) innervation; NPY and VIP were found particularly associated. At the present time, the peptidergic innervation of the prostate seems to play a role of special relevance in prostatic physiology (Dixon *et al*., 2000; Ventura *et al*., 2002). These neuropeptides, behaving as regulators of prostatic secretion, may be involved in modulation of the action of androgens (Gkonos *et al*., 1995; Juarranz *et al*., 2001; Ventura *et al*., 2002). Some studies associate VIP with the proliferation of prostatic acini in rats (Juarranz *et al*., 2001). It is also important to note the post-pubertal decrease of NPY immunoreactive periglandular fibres (Rodriguez *et al*., 2005). This lessening could be attributed to changes due to aging in the periprostatic ganglia (Cowen, 1993).

The relationship among serotonin, NPY and VIP has been evidenced from a functional point of view. VIP and serotonin increase the intracellular level of cyclic-AMP in the prostate epithelium, whereas NPY diminishes it (Gkonos *et al*., 1995). Furthermore, it has been demonstrated that there is neuroendocrine differentiation in-vitro subsequent to the increase of cyclic-AMP (Cox *et al*., 1999).

Another relevant issue is that not all prostate regions are equally influenced by age in respect of innervation. The peptidergic nerves from ventral, ampular and periductal regions are more age-dependent than the nerves from dorso-lateral regions.

In summary: a) discriminant analysis confirms the androgen-dependence of both neuroendocrine cells and peptidergic innervation during the postnatal development of the rat prostate; b) periglandular innervation has more relevance than interglandular innervation in order to classify rats in age groups; and the peptidergic nerves from ventral, ampullar and periductal regions are more age-dependent than the nerves from dorso-lateral regions; c) the peptidergic nerves from ventral, ampullar and periductal regions are more age-dependent than the nerves from the dorso-lateral region.

REFERENCES

Abdul M, Logothetis CJ, Hoosein NM (1995). Growth-inhibitory effects of serotonin uptake inhibitors on human prostate carcinoma cell lines. J Urol 154:247-50.

Abrahamsson PA (1999). Neuroendocrine differentiation in prostatic carcinoma. Prostate 39:135-48.

Adrian TE, Gu J, Allen JM, Tatemoto K, Polak JM, Bloom SR (1984). Neuropeptide Y in the human male genital tract. Life Sci 35:2643-8.

Bjugn R, Gundersen HJ (1993). Estimate of the total number of neurons and glial and endothelial cells in the rat spinal cord by means of the optical disector. J Comp Neurol 328:406-14.

Cohen RJ, Glezerson G, Haffejee Z (1991). Neuro-endocrine cells--a new prognostic parameter in prostate cancer. Br J Urol 68:258-62.

Cowen T (1993). Ageing in the autonomic nervous system: a result of nerve-target interactions? A review. Mech Ageing Dev 68:163-73.

Cox ME, Deeble PD, Lakhani S, Parsons SJ (1999). Acquisition of neuroendocrine characteristics by prostate tumor cells is reversible: implications for prostate cancer progression. Cancer Res 59:3821-30.

Crowe R, Chapple CR, Burnstock G (1991). The human prostate gland: a histochemical and immunohisto-chemical study of neuropeptides, serotonin, dopamine beta-hydroxylase and acetylcholinesterase in autonomic nerves and ganglia. Br J Urol 68:53-61.

di Sant'Agnese PA (1992). Neuroendocrine differentiation in carcinoma of the prostate. Diagnostic, prognostic, and therapeutic implications. Cancer 70:254-68.

Dixon JS, Jen PY, Gosling JA (2000). The distribution of vesicular acetylcholine transporter in the human male genitourinary organs and its co-localization with neuropeptide Y and nitric oxide synthase. Neurourol Urodyn 19:185-94.

Farnsworth WE (1999). Prostate stroma: physiology. Prostate 38:60-72.

Gkonos PJ, Krongrad A, Roos BA (1995). Neuroendocrine peptides in the prostate. Urol Res 23:81-7.

Gundersen HJ, Bendtsen TF, Korbo L, Marcussen N, Moller A, Nielsen K, *et al*. (1988). Some new, simple and efficient stereological methods and their use in pathological research and diagnosis. APMIS 96:379-94.

Gundersen HJ, Osterby R (1981). Optimizing sampling efficiency of stereological studies in biology: or 'do more less well!' J Microsc 121:65-73.

Hair JF, Tatham RL, Anderson RE, Black W (1998). Multivariate data analysis, 5 ed. New Jersey: Prentice Hall.

Howard CV, Reed MG (2005). Length estimation. In: Howard CV and Reed MG (eds). Unbiased Stereology: Three-dimensional measurement in microscopy, 2 ed. Oxford: Bios Scientific Publishers, pp. 119-25

Jen PY, Dixon JS, Gosling JA (1996). Co-localisation of tyrosine hydroxylase, nitric oxide synthase and neuro-peptides in neurons of the human postnatal male pelvic ganglia. J Auton Nerv Syst 59:41-50.

Juarranz MG, Bodega G, Prieto JC, Guijarro LG (2001). Vasoactive intestinal peptide (VIP) stimulates rat prostatic epithelial cell proliferation. Prostate 47:285-92.

Lange W, Unger J (1990). Peptidergic innervation within the prostate gland and seminal vesicle. Urol Res 18: 337-40.

Lujan M, Paez A, Llanes L, Angulo J, Berenguer A (1998). Role of autonomic innervation in rat prostatic structure maintenance: a morphometric analysis. J Urol 160:1919-23.

Martin JJ, Martin R, Codesal J, Fraile B, Paniagua R, Santamaria L (2001). Cadmium chloride-induced dysplastic changes in the ventral rat prostate: an immunohistochemical and quantitative study. Prostate 46: 11-20.

Martin R, Fraile B, Peinado F, Arenas MI, Elices M, Alonso L, et al. (2000). Immunohistochemical localization of protein gene product 9.5, ubiquitin, and neuropeptide Y immunoreactivities in epithelial and neuroendocrine cells from normal and hyperplastic human prostate. J Histochem Cytochem 48:1121-30.

Martin R, Nieto S, Santamaria L (1997). Stereologic estimates of volume-weighted mean nuclear volume in colorectal adenocarcinoma: correlation with histologic grading, Dukes' staging, cell proliferation activity and p53 protein expression. Gen Diagn Pathol 143:29-38.

Mayhew TM (1991). The new stereological methods for interpreting functional morphology from slices of cells and organs. Exp Physiol 76:639-65.

Mayhew TM, Gundersen HJ (1996). If you assume, you can make an ass out of u and me': a decade of the disector for stereological counting of particles in 3D space. J Anat 188(1):1-15.

McVary KT, McKenna KE, Lee C (1998). Prostate innervation. Prostate Suppl 8:2-13.

McVary KT, Razzaq A, Lee C, Venegas MF, Rademaker A, McKenna KE (1994). Growth of the rat prostate gland is facilitated by the autonomic nervous system. Biol Reprod 51:99-107.

Mottet N, Costa P, Bali JP (1999). Autonomic nervous system and prostatic physiology. Specific features of the alpha-adrenergic system. Prog Urol 9:26-36.

Rodriguez R, Pozuelo JM, Martin R, Arriazu R, Santamaria L (2005). Stereological quantification of nerve fibers immunoreactive to PGP 9.5, NPY, and VIP in rat prostate during postnatal development. J Androl 26: 197-204.

Rodriguez R, Pozuelo JM, Martin R, Henriques-Gil N, Haro M, Arriazu R, et al. (2003). Presence of neuroendocrine cells during postnatal development in rat prostate: Immunohistochemical, molecular, and quantitative study. Prostate 57:176-85.

Sterio DC (1984). The unbiased estimation of number and sizes of arbitrary particles using the disector. J Microsc 134(2):127-36.

Ventura S, Pennefather J, Mitchelson F (2002). Cholinergic innervation and function in the prostate gland. Pharmacol Ther 94:93-112.

Wanke IE, Huang M, Rorstad OP (1990). Selective effect of castration on the anterior pituitary VIP receptor of male rats. Peptides 11:1157-61.

Wreford NG (1995). Theory and practice of stereological techniques applied to the estimation of cell number and nuclear volume in the testis. Microsc Res Tech 32: 423-36.